

## Flow-Induced Noise from a Sharp-Edged Flat Plate Using a Quasi-Periodic CFD-BEM Technique

M. Karimi<sup>1</sup>, P. Croaker<sup>1</sup>, N. Kessissoglou<sup>1</sup>, C. Doolan<sup>2</sup> and S. Marburg<sup>3</sup>

<sup>1</sup>School of Mechanical and Manufacturing Engineering, UNSW Australia, Sydney, Australia

<sup>2</sup>School of Mechanical Engineering, The University of Adelaide, Adelaide, Australia

<sup>3</sup>LRT4-Institute of Mechanics, Universität der Bundeswehr München, D-85579 Neubiberg, Germany

### Abstract

The flow-induced noise from a sharp-edged flat plate submerged in low Mach number flow is predicted using a quasi-periodic computational fluid dynamics (CFD)-boundary element method (BEM) technique. A high-order reconstruction scheme is used to extract acoustic sources based on Lighthill's analogy from the flow field data. Acoustic waves generated by these flow noise sources propagate to and are scattered by the trailing edge of the plate. The fluctuating flow field is obtained using an incompressible CFD solver. A BEM model of the sharp-edged flat plate is used to predict the scattered sound pressure field. A quasi-periodic technique is implemented in the BEM model so that the sound generated by the entire span of the plate can be predicted by modelling only a small spanwise segment. The computed aerodynamic and acoustic results are compared with experimental data obtained using the anechoic wind tunnel at the University of Adelaide.

### Introduction

Hybrid large eddy simulation (LES) - acoustic analogy techniques have been developed that provide a high fidelity approach to predict the interaction of flow induced noise with a body submerged in the flow. The LES simulations are able to capture the flow noise sources with great detail over a wide range of frequencies and this leads to accurate acoustic predictions. Wang and Moin [13] performed an incompressible large eddy simulation of turbulent flow over a flat strut, with the predicted hydrodynamics comparing well with the experiments conducted by Blake [1]. Wang et al. [14] conducted a similar hybrid LES - acoustic analogy simulation on the cambered airfoil of an industrial fan blade. Seo and Moon [12] developed a modified version of the perturbed compressible equations known as the linearised perturbed compressible equation (LPCE). They showed that the LPCE method can accurately predict the sound pressure field radiated from turbulent flow past a cylinder.

Wolf and Lele [15] developed a hybrid technique based on compressible LES simulation of the flow field, coupled with the FWH acoustic analogy to predict the radiated field. Their approach uses both the fluctuating surface pressures and volume quadrupole sources calculated during the LES simulation to drive the subsequent acoustic propagation analysis. They make no assumptions about the compactness of the acoustic source region, nor on the shape of the scattering surface. Moreau et al. [9, 10] conducted a number of aeroacoustic experiments on sharp-edged flat plates in an anechoic wind tunnel at low-to-moderate Reynolds number. They examined a variety of semi-empirical methods for predicting trailing edge noise which were shown to underestimate noise at lower frequencies [9].

Lee and Cheong [5] developed an efficient methodology for frequency-domain prediction of broadband trailing edge noise from a blunt flat plate. They used a semi-analytical model to specify the incident pressure spectrum. They then applied a point pressure spectrum within the boundary layer as the input

for prediction of the broadband trailing edge noise. Khalighi et al. [4] developed a boundary integral equation from Lighthill's wave equation which was solved using BEM. The method was applied to predict the sound pressure field radiated by turbulent flow past a cylinder and an automotive side mirror, as well as the trailing edge noise from an airfoil [3].

In this work, the self-generated noise from a sharp-edged flat plate submerged in low Mach number flow is predicted using a quasi-periodic CFD-BEM technique. The unsteady incompressible flow field past a flat plate with a sharp trailing edge is simulated using an LES method. The acoustic field is then computed using Lighthill's analogy by extracting sources from the unsteady flow data. Finally, the incident acoustic field is applied to a quasi-periodic BEM model based on the Burton-Miller formulation to predict the scattered sound pressure. The quasi-periodic technique predicts the sound generated by the entire span of the plate by modelling only a small spanwise segment.

### Acoustic Formulation

#### Boundary Element Method

The non-homogeneous Helmholtz equation is given by

$$\Delta p(\mathbf{x}) + k^2 p(\mathbf{x}) = -F \quad (1)$$

where  $p(\mathbf{x})$  is the acoustic pressure at field point  $\mathbf{x}$ ,  $F$  is the source,  $\Delta$  is the Laplacian operator,  $k = \omega/c$  is the acoustic wave number,  $\omega$  is the angular frequency and  $c$  is the speed of sound. The non-homogenous Helmholtz equation can be written in a weak formulation after integrating by parts twice as follows [8]

$$c(\mathbf{x})p(\mathbf{x}) + \int_{\Gamma} \frac{\partial G(\mathbf{x}, \mathbf{y})}{\partial n(\mathbf{y})} p(\mathbf{y}) d\Gamma(\mathbf{y}) = \tilde{i}\omega\rho_0 \int_{\Gamma} G(\mathbf{x}, \mathbf{y}) v_f(\mathbf{y}) d\Gamma(\mathbf{y}) + p_{\text{inc}}(\mathbf{x}) \quad (2)$$

where  $\rho_0$  is fluid density and  $\tilde{i} = \sqrt{-1}$  is the imaginary unit. The vector  $\mathbf{n}(\mathbf{y})$  represents the outward normal vector at the point  $\mathbf{y}$ ,  $\partial/\partial n(\mathbf{y})$  is the normal derivative and  $\mathbf{y}$  is a source point position on the boundary  $\Gamma$ . Solution of the non-homogenous Helmholtz equation can be obtained by calculating the incident acoustic pressure radiated by the source and applying it as a load to the boundary integral equation (2).  $p_{\text{inc}}(\mathbf{x})$  is the incident acoustic pressure as a result of the acoustic source.  $c(\mathbf{x})$  is a free-term coefficient and equals 1 in the domain interior and 0.5 on a smooth boundary.  $G(\mathbf{x}, \mathbf{y})$  is the free-space Green's function for the Helmholtz equation given by

$$G(\mathbf{x}, \mathbf{y}) = \frac{e^{i\tilde{i}kr}}{4\pi r} \quad \text{where} \quad r = |\mathbf{x} - \mathbf{y}| \quad (3)$$

The fluid particle velocity  $v_f(\mathbf{x})$  is related to the normal derivative of the acoustic pressure as follows

$$v_f(\mathbf{x}) = \frac{1}{\tilde{i}\omega\rho_0} \frac{\partial p(\mathbf{x})}{\partial n(\mathbf{x})} \quad (4)$$

It has been demonstrated that equation (2) has a major flaw for exterior acoustic applications; that is, it fails to have a unique solution at certain so-called irregular frequencies [7]. Burton and Miller [2] showed that a remedy to this problem is to use the linear combination of equation (2) in conjunction with its differentiated form. This will lead to a unique solution for exterior acoustic problems at all frequencies.

### Flow-Generated Sound Sources

For flow-induced noise problems [6], the source  $F$  in equation (1) can be replaced with

$$F = \frac{\partial^2 T_{ij}}{\partial y_i \partial y_j} \quad (5)$$

where  $T_{ij} = \rho_0 u_i u_j$  is the approximate Lighthill's tensor (at low Mach number), and  $u_i, u_j$  are respectively the  $i^{\text{th}}$  and  $j^{\text{th}}$  components of the velocity vector. The particular solution of the non-homogenous Helmholtz equation due to this source can be expressed by

$$p_{\text{inc}}(\mathbf{x}) = \int_{\Omega} \frac{\partial^2 T_{ij}(\mathbf{y})}{\partial y_i \partial y_j} G(\mathbf{x}, \mathbf{y}) d\mathbf{y} \quad (6)$$

where  $\Omega$  is the acoustic domain. In this study, the sound pressure must satisfy the Sommerfeld radiation condition in the far field as well as the Neumann boundary condition on the surface of the plate. The latter condition implies that the plate is considered rigid with zero admittance. Therefore, the boundary condition can be expressed as follows

$$v_f(\mathbf{y}) = 0, \quad \mathbf{y} \in \Gamma \quad (7)$$

### Quasi-Periodic Boundary Element Technique

A quasi-periodic technique is implemented in the BEM model so that the sound generated by the entire surface of a body can be predicted by modelling only a small segment of the body. To do this, the surface of the body is divided into  $(2N + 1)$  sections. Hence, the total length of the body is given by

$$L = (2N + 1)x_p \quad (8)$$

where  $x_p$  is the length of each section.  $N$  is the number of sections on each side of the middle section  $\Gamma_0$ .

A periodic solution for the acoustic pressure given by  $p(\mathbf{y}) = p(\mathbf{y} + n\mathbf{d})$  is assumed, where  $\mathbf{d}$  is a vector from a collocation point of one boundary section to its adjacent boundary section. The length of  $\mathbf{d}$  is equal to  $x_p$ .

With the assumption of a periodic solution as well as considering the Neumann boundary condition, equation (2) and its differentiated form can be respectively rewritten as follows

$$c(\mathbf{x})p(\mathbf{x}) + \sum_{n=-N}^N \left[ \int_{\Gamma_n} \frac{\partial G(\mathbf{x}, \mathbf{y}_n)}{\partial n(\mathbf{y}_n)} p(\mathbf{y}) d\Gamma_n(\mathbf{y}_n) \right] = p_{\text{inc}}(\mathbf{x}) \quad (9)$$

$$\sum_{n=-N}^N \left[ \int_{\Gamma_n} \frac{\partial^2 G(\mathbf{x}, \mathbf{y}_n)}{\partial n(\mathbf{x}) \partial n(\mathbf{y}_n)} p(\mathbf{y}) d\Gamma_n(\mathbf{y}_n) \right] = \frac{\partial p_{\text{inc}}(\mathbf{x})}{\partial n(\mathbf{x})} \quad (10)$$

The acoustic pressure on each element can be discretised as follows

$$p(\mathbf{y}) = \sum_{i=1}^M \Phi_i(\mathbf{y}) p_i \quad (11)$$

where  $\Phi_i(\mathbf{y})$  are interpolation functions and  $p_i$  represents the sound pressure at nodal points. In the case of a quasi-periodic assumption, only collocation points of the elements located on  $\Gamma_0$  need to be included in the computation. This is sufficient since the quasi-periodic assumption leads to a situation where collocation points of other sections only provide redundant information. The quasi-periodic BEM formulation based on the Burton and Miller method is obtained as the following linear system of equations

$$(\mathbf{H} + \beta \mathbf{D})\mathbf{p} = \mathbf{p}_{\text{inc}} + \beta \mathbf{q}_{\text{inc}} \quad (12)$$

where  $\mathbf{q}_{\text{inc}}$  represents the incident pressure gradient vector and  $\beta$  is the coupling parameter in the Burton and Miller formulation. Using this quasi-periodic BEM model, the acoustic pressure  $p$  radiated from flow sources and scattered by the body is predicted.

### Fluid Dynamics Simulation

To validate the approach adopted in this work, a flat plate model was used which corresponds to the experiment conducted by Moreau et al. [9] in an anechoic wind tunnel. The flat plate used in both the experiment and simulation has a chord of 200 mm, a span of 450 mm and a thickness of 5 mm. The leading edge is circular with a diameter of 5 mm while the trailing edge is a symmetric wedge shape with an apex angle of  $12^\circ$ , as shown in figure 1. In the experimental test, the flat plate was tested with zero angle of attack and the radiated sound pressure was measured at three positions, one above the trailing edge, one below the trailing edge and one above the leading edge.

An incompressible flow field past the flat plate is simulated at a Reynolds number based on chord  $Re_c = 2.0 \times 10^5$  and Mach number  $M = 0.044$ . At this Reynolds number the flow is in the turbulent unsteady regime and is three dimensional. The LES simulation is performed in Fluent on a C-grid domain with nearly 3 million hexahedral cells. A relatively large computational domain is used to minimize the boundary condition influence, which is extended two chords above and below the plate as well as upstream and downstream. A sponge layer extends the computational domain in the downstream direction for an additional chord. The mesh distribution is biased so that the region near the plate and also the wake region contains a high cell density to resolve eddies and fluctuations. Apart from the vicinity of the leading edge, the resolution of the near-wall grid on the plate is  $\Delta x^+ \leq 29$ ,  $\Delta y^+ \leq 1$  and  $\Delta z^+ \leq 4.7$ . The cell size in the sponge layer grows rapidly in the  $x$ -direction. The sponge layer is implemented to allow the vortical disturbances in the wake to leave the computational domain smoothly. This is achieved by defining a cosine function of  $x$  which increases the viscosity through the layer.

The inlet velocity is set to 15 m/s on the semi-circular boundary, while a zero average pressure is imposed at the outlet. A no-slip condition is applied on the surface of the plate, and the top and bottom boundaries are considered as free-slip walls. It should be noted that a spanwise extension is selected as 3% of the plate chord with flow periodicity assumed at the side boundaries. The calculation procedure is described as follows. A transient simulation based on Menter's shear-stress transport (SST)  $k - \omega$  model is initially conducted as an initial condition for the LES.

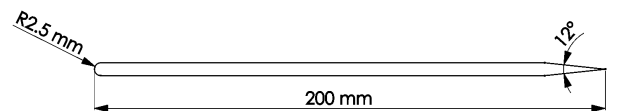


Figure 1: Flat plate dimensions

Velocity components from the LES are then extracted to calculate the sound sources. Since these sources are in the time domain, a discrete Fourier transform (DFT) is performed to transfer the data into the frequency domain. Once the incident pressure and its gradient are obtained, the total sound pressure can be computed from the BEM formulation given by equation (12).

## Results and Discussion

### Turbulent Flow at the Trailing Edge

Figure 2 compares the mean and fluctuating velocity profiles extracted from the LES simulation with results obtained experimentally from wind tunnel measurements at the University of Adelaide, where  $c$  is the plate chord,  $U_\infty$  is the free-stream velocity and  $U$  is the mean velocity. The velocity was measured in the vertical direction  $y$  at a constant  $x$  position of 0.7 mm from trailing edge. Figure 2 reveals that the velocity profiles for the current flat plate model are mostly symmetric about the trailing edge. Good agreement between numerical results obtained in this work and experimental results by Moreau et al. [9] can be observed in figure 2(a). The computed root-mean-square (RMS) fluctuating velocity is compared with experimental results in figure 2(b), where  $u'$  is the fluctuating velocity. The current LES model overpredicts the fluctuating velocity at the region near the trailing edge ( $-0.2 < y/c < 0.2$ ), beyond this region the fluctuating velocity is lower than experimental values.

The spectra of fluctuating velocity are presented in figure 3 at two different positions in the wake of the flat plate. Figure 3(a) shows the velocity spectra adjacent to the trailing edge. For this case the CFD results are in very good agreement with experimental data. At a position further from the trailing edge as shown in figure 3(b) the CFD results diverge from experimental data at frequencies above around 2 kHz. This discrepancy can be attributed to the mesh distribution in the downstream region. The cell size in the mesh increases in the  $x$ -direction. Hence, at a position further from the trailing edge, the grid resolution was not sufficient to appropriately predict the velocity fluctuation at high frequencies. A similar behaviour can also be observed from figures 4 and 5, which show the spectral maps of the fluctuating velocity measured in the wake in the streamwise direction and in the vertical direction, respectively. Both spectral maps indicate that the power spectral density of the fluctuating velocity is well predicted near the trailing edge for the entire range of frequencies. Nevertheless, as the measuring point moves from vicinity of the trailing edge, the accuracy of the results decreases due to the gradual growth of the grid size.

### Frequency Spectra of the Far-Field Noise

The broadband noise radiated by the flat plate predicted using the quasi-periodic boundary element method is compared with experimental results in figure 6. The sound pressure is computed at two positions corresponding to above and below the trailing edge, which are the locations of microphones in the experiment [10]. Figure 6 shows that the numerical results are in good agreement with experimental data at high frequencies. However, there is a considerable difference between the numerical and experimental results at low frequencies. According to the Corcos model [11], the spanwise coherence length can be estimated by  $L_c(\omega) \approx 2.1U_c/\omega$ , where  $U_c$  is the convection speed. According to this model and considering the fact that the segment length used in the CFD simulation was only 3% of the plate chord (6 mm), the current simulated segment length cannot resolve the correct behaviour of the flow structures with frequencies less than 670 Hz. To obtain reasonable results at all frequencies between 300 Hz and 4 kHz, the minimum span of 14 mm should be implemented in the simulation. However, using the current

span it is possible to reasonably predict the sound pressure at high frequencies.

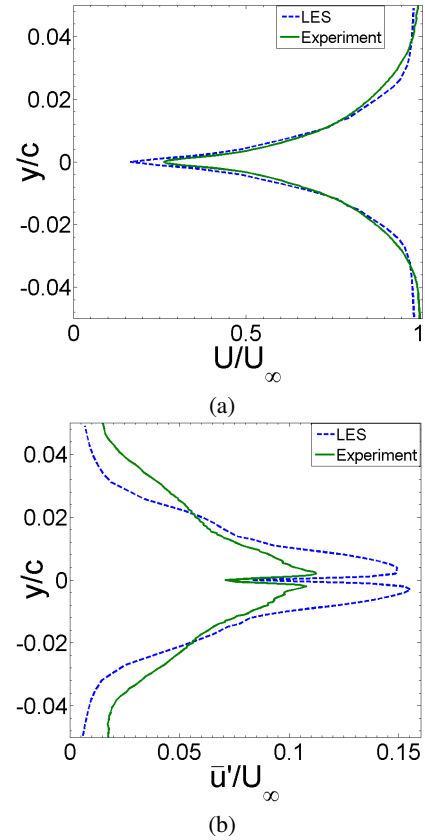


Figure 2: Normalized velocity measured in the near wake of the flat plate; (a) Normalized mean velocity  $U/U_\infty$  and (b) Normalized RMS velocity fluctuations  $\bar{u}'/U_\infty$

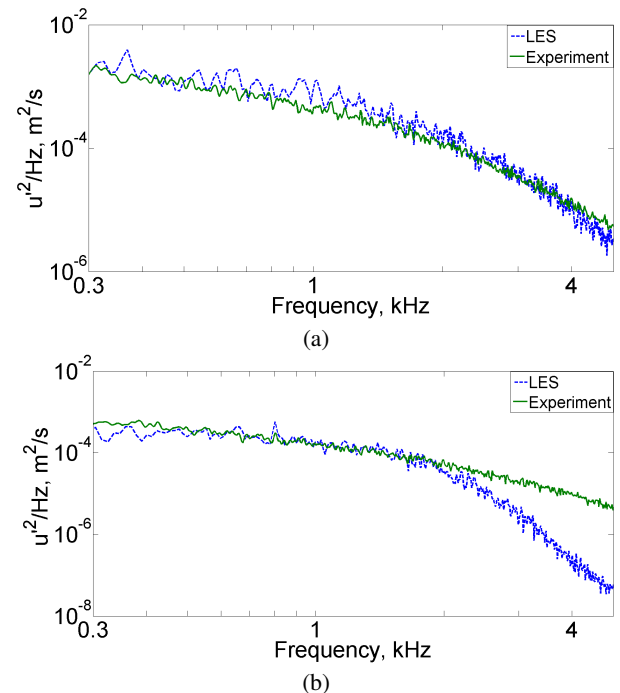
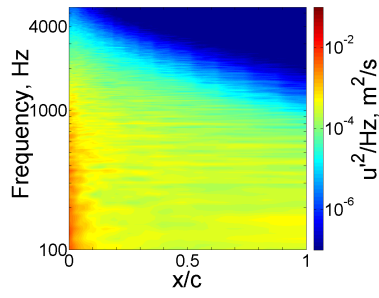
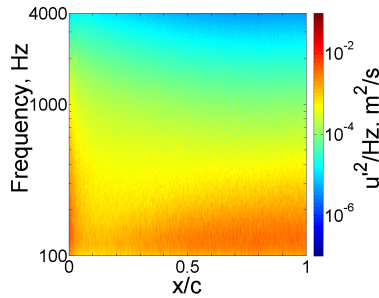


Figure 3: The velocity spectra for the flat plate near the trailing edge at  $y/c=-0.0035$ ; (a)  $x/c=0.01$  and (b)  $x/c=0.2$

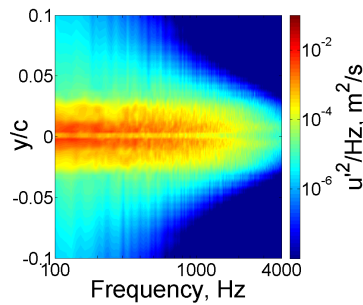


(a)

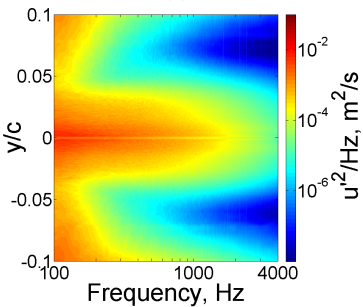


(b)

Figure 4: Spectral maps of the power spectral density of the fluctuating velocity measured in the streamwise ( $x$ ) direction at  $y/c=-0.0035$ ; (a) LES results and (b) experimental results



(a)



(b)

Figure 5: Spectral maps of the power spectral density of the fluctuating velocity measured near the trailing edge in the vertical direction at  $x/c=0.0035$ ; (a) LES results and (b) experimental results

### Concluding Remarks

In this work, the flow-induced noise from a sharp-edged flat plate submerged in low Mach number flow using a quasi-periodic CFD-BEM technique has been presented. The fluctuating flow field was obtained using an incompressible CFD solver. A quasi-periodic BEM model of the sharp-edged flat plate was implemented so that the sound generated by the entire span of the plate was predicted by modelling only a small spanwise segment. The computed acoustic results are compared with experimental data obtained using the anechoic wind tunnel at the University of Adelaide. The results from this study suggests that a finer mesh is required to accurately predict the flow fluctuation in the wake at high frequencies. Furthermore, a longer span should be

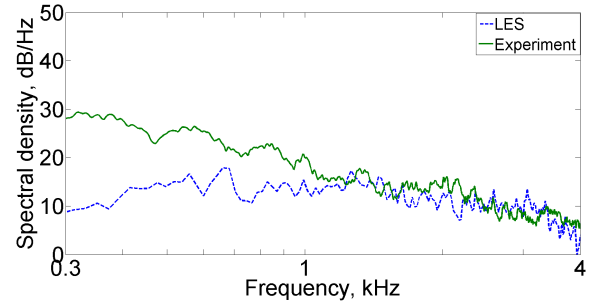


Figure 6: Comparison of experimental and numerical far-field acoustic spectra

modelled in the simulation to capture the flow features at low frequencies.

### References

- [1] Blake, W. K., A statistical description of pressure and velocity fields at the trailing edge of a flat strut, DTNSRDC report 4241, David Taylor Naval Ship R & D Center, Maryland, 1975.
- [2] Burton, A. J. and Miller, G. F., The application of integral equation methods to the numerical solution of some exterior boundary-value problems, *Proc Roy Soc Lon Ser A*, **323**, 1971, 201–210.
- [3] Khalighi, Y., *Computational Aeroacoustics of Complex Flows at Low Mach Number*, Ph.D. thesis, Stanford University, 2010.
- [4] Khalighi, Y., Mani, A., Ham, F. and Moin, P., Prediction of sound generated by complex flows at low mach numbers, *AIAA J*, **48**, 2010, 306–316.
- [5] Lee, G.-S. and Cheong, C., Frequency-domain prediction of broadband trailing edge noise from a blunt flat plate, *J Sound Vib*, **332**, 2013, 5322–5344.
- [6] Lighthill, M. J., On sound generated aerodynamically, *Proc Soc Roy Soc A*, **211**, 1952, 564–587.
- [7] Marburg, S. and Amini, S., Cat's eye radiation with boundary elements: Comparative study on treatment, *J Comput Acoust*, **13**, 2005, 21–45.
- [8] Marburg, S. and Nolte, B., *Computational acoustics of noise propagation in fluids - Finite and boundary element methods*, Springer, 2008.
- [9] Moreau, D. J., Brooks, L. and Doolan, C. J., Broadband trailing edge noise from a sharp-edged strut, *J Acoust Soc Am*, **129**, 2011, 2820–9.
- [10] Moreau, D. J., Brooks, L. and Doolan, C. J., The effect of boundary layer type on trailing edge noise from sharp-edged flat plates at low-to-moderate Reynolds number, *J Sound Vib*, **331**, 2012, 3976–3988.
- [11] Roger, M. and Moreau, S., Broadband self-noise from loaded fan blades, *AIAA J*, **42**, 2004, 536–544.
- [12] Seo, J. and Moon, Y., Aerodynamic noise prediction for long-span bodies, *J Sound Vib*, **306**, 2007, 564–579.
- [13] Wang, M. and Moin, P., Computation of trailing-edge flow and noise using large-eddy simulation, *AIAA J*, **38**, 2000, 2201–2209.
- [14] Wang, M., Moreau, S., Iaccarino, G. and Roger, M., LES prediction of wall-pressure fluctuations and noise of a low-speed airfoil, *Int J Aeroacoust*, **8**, 2009, 177–198.
- [15] Wolf, W. R. and Lele, S. K., Trailing-edge noise predictions using compressible large eddy simulation and acoustic analogy, *AIAA J*, 2423–2434.